Lab Assignment 4: Inverted Pendulum

Team members:
Shiva Ghose, @gshiva
John Peterson, @jrpeters
Peter Turpel, @pturpel
Chan-Rong Lin, @pmelin

Teamwork Participation Pledge :: Team 1

I attest that I have made a fair and equitable contribution to this lab and submitted assignment.

My signature also indicates that I have followed the University of Michigan Honor Code, while working on this lab and assignment.

I accept my responsibility to look after all of the equipment assigned to me and my team, and that I have read and understood the X50 Lab Rules.

Name	Email	Signature
Shiva Ghose	gshiva@umich.edu	
John Peterson	jrpeters@umich.edu	
Peter Turpel	pturpel@umich.edu	
Chan-Rong Lin	pmelin@umich.edu	

1 System Modeling

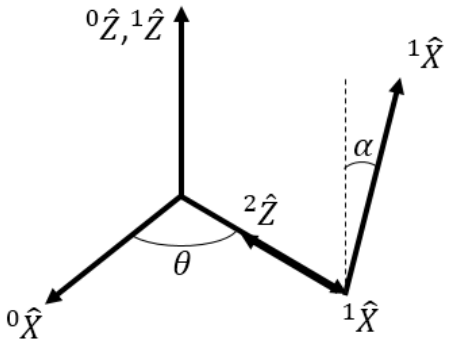

Figure 1: The co-ordinate frames of the inverted pendulum system

a. Physical Model

We model the physical system as a pair of rigid links, the horizontal arm and the pendulum mounted to the end of the arm, neglecting the presence of the encoder cable, using a lumped parameter model.

b. Assumptions

We make the following assumptions while modeling the system:

- All of the links are rigid - this allows us to neglect work done by the internal constraining forces of the system such as internal losses due to collisions and deformations. This assumption very nearly holds because system is built using stiff metals and bearings that are well fitted.
- Air resistance is neglected - this is due to the small cross sectional areas and low velocities experienced by the system. Additionally this is neglected due to the difficulty in constructing an appropriate model for these losses and determining its forces.
- The axis of rotation of the horizontal arm is fixed in space and perfectly level with the ground - this assumption overlaps with neglecting losses due to internal constraints and ensures that there will be no potential energy term associated with the arm and avoids the need to consider the motor stand, the table beneath it etc.
- The presence of the encoder cable connected to the arm is neglected - We found that the cable has a large impact on our system however its influence would be very difficult to model because it is not fixed to the arm and because the forces it introduces are highly non linear.

Apart from the above list, the standard set of control systems assumptions are also made:

- The current driver acts instantaneously - the transients involved occur so quickly with respect to the system response time that we virtually have immediate response. Also, the motor, acting as a low pass filter, will reject the high frequency components of the driver.
- The DAQ has instantaneous and correct response - we ignore the quantization and discretization errors of the DAQ and further assume that offset errors have been accounted for. This is valid because our control loop runs at 100 Hz while the DAQ can be sampled at 1000 Hz. Additionally we believe that the DAQ has been calibrated and static errors have been removed.

c. Mathematical Modeling

Forwards Kinematics

Let ${}^0F$ represent the fixed world coordinate frame, with $\mathbf{{}^0\hat{z}}$ aligned with the motor shaft and with $\mathbf{{}^0\hat{x}}$ pointing along the initial direction of the horizontal arm when the system is initialized (as seen in figure 1 on page 2). Let the origin of ${}^0F$ be located to coincide with the motor axis and the axis of rotation of the pendulum. Let ${}^1F$, representing the local frame of the horizontal arm, be attached to the horizontal arm, with $\mathbf{{}^1\hat{z}}$ aligned with the motor shaft and $\mathbf{{}^1\hat{x}}$ aligned with the motor arm pointed towards the pendulum. Let ${}^2F$ be located such that its origin is along $\mathbf{{}^1\hat{x}}$ at a distance l_1, with $\mathbf{{}^2\hat{x}}$ pointing along the pendulum and $\mathbf{{}^2\hat{z}}$ along the $-\mathbf{{}^1\hat{x}}$ direction. Where l_1 is the distance from the axis of rotation of the motor to the center of mass of the pendulum along the $\mathbf{{}^1\hat{x}}$ direction. Let θ denote the angle between $\mathbf{{}^0\hat{x}}$ and $\mathbf{{}^1\hat{x}}$ and let α denote the angle between $\mathbf{{}^1\hat{z}}$ and $\mathbf{{}^2\hat{x}}$ measured clockwise when viewed from $\mathbf{{}^1\hat{x}}$. We assume that the motor and the horizontal arm are rigidly connected and can be treated as a single inertia for purposes of our energy calculations below.

Then:

$$ {}^0F = R_z(\theta)T_x(l_1)R_y(-\pi/2)R_z(\alpha)\left({}^2F\right) $$

Let l_{2c} be the distance along $\mathbf{{}^2x}$ from the origin of ${}^2F$ to the center of mass of the pendulum. Then the location of the center of mass of the pendulum in the world coordinate system $\mathbf{{}^0P_{2c}}$ is given as:

$$ \mathbf{{}^0P_{2c}} = R_z(\theta)T_x(l_1)R_y(-\pi/2)R_z(\alpha)\left(\mathbf{{}^2P_{2c}}\right) = R_z(\theta)T_x(l_1)R_y(-\pi/2)R_z(\alpha)\left[l_{2c},0,0\right]^T $$

$$ \mathbf{{}^0P_{2c}} = \begin{bmatrix} -l_{2c}\sin(\theta)\sin(\alpha) + l_1\cos(\theta) \\ l_{2c}\cos(\theta)\sin(\alpha) + l_1\sin(\theta) \\ l_{2c}\cos(\alpha) \end{bmatrix} $$

From this position we can then determine the linear velocity of the center of mass of the pendulum in the world frame denoted $\mathbf{{}^0\dot{P}_{2c}}$. Let J denote the matrix of partial derivatives of $\mathbf{{}^0P_{2c}}$ with respect to θ and α. Then the $\mathbf{{}^0\dot{P}_{2c}}$ is given by.

$$ \mathbf{{}^0\dot{P}_{2c}} = J\begin{bmatrix} \dot{\theta} \\ \dot{\alpha} \end{bmatrix} = \begin{bmatrix} -l_{2c}sin(\alpha)\cos(\theta) - l_1\sin(\theta) & -l_{2c}\sin(\theta)\cos(\alpha) \\ -l_{2c}sin(\alpha)\sin(\theta) + l_1\cos(\theta) & l_{2c}\cos(\theta)\cos(\alpha) \\ 0 & -l_{2c}\sin(\alpha) \end{bmatrix}\begin{bmatrix} \dot{\theta} \\ \dot{\alpha} \end{bmatrix} $$

We can also determine the angular velocity of the pendulum about its center of mass in the pendulum fixed frame ${}^2F$ by the following:

$$ \omega_{\mathbf{2}} = \dot{\theta}(\mathbf{{}^1\hat{z}}) + \dot{\alpha}(\mathbf{{}^2\hat{z}}) = (R_y(-\pi/2)R_z(\alpha))^{-1}\left[0,0,\dot{\theta}\right]^T + \dot{\alpha}(\mathbf{{}^2\hat{z}}) $$

$$ \mathbf{{}^2}\omega_{\mathbf{2}} = \begin{bmatrix} \dot{\theta}\cos(\alpha) \\ -\dot{\theta}\sin(\alpha) \\ \dot{\alpha} \end{bmatrix} $$

Rather than concern our selves with the forwards kinematics of the horizontal arm, because we assume that its only motion is a rotation about $\mathbf{{}^0\hat{z}}$ which allows us to simply apply the parallel axis theorem to obtain its moment of inertia

System Energy

Our system is composed of two rigid bodies, then the horizontal arm and the pendulum. Each has an energy denoted E_1 and E_2 respectively. Using the forwards kinematics derived above we can compute the kinetic and potential energies associated with each body as a function of θ, α, $\dot{\theta}$, and $\dot{\alpha}$.

$$E_1 = T_1 + V_1 \qquad E_2 = T_2 + V_2$$

By our assumption above that ${}^{\mathbf{1}}\hat{\mathbf{z}}$ is parallel to the direction of gravity, the term V_1 can be taken to be 0. Furthermore, rather than expand T_1 into linear and rotational components, we can simply use a single rotation term with a modified moment of inertia, I_{1z1}. Let l_{1c} be the distance along ${}^{\mathbf{1}}\hat{\mathbf{x}}$ from the origin to the center of mass of the rotor ${}^{1}P_{1c}$, and let m_1 be the mass of the horizontal arm. Note that we must also include the rotor inertia :

$$E_1 = I_{1z1}\dot{\theta}^2 = \left(I_{1zzc} + I_{rotor} + m_1 l_{1c}^2\right)\dot{\theta}^2$$

The expression for E_2 is much more complex, we will break the kinetic energy into a translational and a rotational component.

Because the pendulum is perpendicular to the horizontal arm which is perpendicular to the ground, the potential energy of the pendulum, V_2 only depends on alpha, the distance from the axis of rotation to the center of mass along ${}^{\mathbf{2}}\hat{\mathbf{x}}$, l_{2c}, the mass of the pendulum, m_2, and the acceleration due to gravity, g. Without loss of generality, we assume that zero potential energy occurs for $\alpha = 0$.

$$V_2 = \left(\cos(\alpha) - 1\right) l_{2c} m_2 g$$

The translation kinetic energy of the pendulum T_{2T} is given by the following expression:

$$T_{2T} = \frac{1}{2}m_2\left({}^{\mathbf{0}}\dot{\mathbf{P}}_{\mathbf{2c}}\right)^2 = \frac{1}{2}m_2\left({}^{\mathbf{0}}\dot{\mathbf{P}}_{\mathbf{2c}}\right)^T\left({}^{\mathbf{0}}\dot{\mathbf{P}}_{\mathbf{2c}}\right) = \frac{1}{2}m_2\left[\dot{\theta},\dot{\alpha}\right]J^T J\begin{bmatrix}\dot{\theta}\\ \dot{\alpha}\end{bmatrix}$$

$$T_{2T} = \dot{\theta}^2\left(l_{2c}^2\sin^2(\alpha) + l_1^2\right) + 2l_1 l_{2c}\dot{\theta}\dot{\alpha}\cos(\alpha) + \left(\dot{\alpha}l_{2c}\right)^2$$

The rotational kinetic energy of the pendulum is given by the following expression where I_2 is the 3 by 3 moment of inertia tensor of the pendulum.

$$T_{2R} = \frac{1}{2}{}^{\mathbf{2}}\omega_{\mathbf{2}}{}^T I_2{}^{\mathbf{2}}\omega_{\mathbf{2}} = \frac{1}{2}\left[\dot{\theta}^2\left(I_{2xx}\cos^2(\alpha) - 2I_{2xy}\sin(\alpha)\cos(\alpha) + I_{2yy}\sin^2(\alpha)\right) + 2I_{2xz}\dot{\theta}\dot{\alpha}\sin(\alpha) + I_{2zz}\dot{\alpha}^2\right]$$

Note this is where the arbitrary sign flip is!!!

As discussed later I_{2xy} and I_{2yz} are very nearly 0 and have been neglected for the rest of the derivation.

$$T_{2R} = \frac{1}{2}\left[\dot{\theta}^2\left(I_{2xx}\cos^2(\alpha) + I_{2yy}\sin^2(\alpha)\right) + I_{2zz}\dot{\alpha}^2\right] - I_{2xz}\dot{\theta}\dot{\alpha}\cos(\alpha)$$

Lagrange's Equation and non-Linear Equations of Motion

The Lagrange method can be used to compute the equations of motion of complex dynamical systems using the total system energy derived above along with the generalized coordinates of the system q_i and generalized non-conservative forces on the system Q_{NCi}. These non-conservative forces are the damping forces exerted on both the pendulum and the horizontal arm determined by b_α and b_θ respectively, the motor torque exerted on the horizontal arm, τ_m, and the force of coulomb friction exerted on both the pendulum and the horizontal arm denoted $\tau_{C\alpha}$ and $\tau_{C\theta}$ respectively.

$$\begin{aligned}\frac{d}{dt}\frac{\partial\mathcal{L}}{\partial\dot{q}_i} - \frac{\partial\mathcal{L}}{\partial q_i} &= Q_{NCi}\\ \frac{d}{dt}\frac{\partial\mathcal{L}}{\partial\dot{\theta}} - \frac{\partial\mathcal{L}}{\partial\theta} &= -b_\theta\dot{\theta} + \tau_m + \tau_{C\theta}\\ \frac{d}{dt}\frac{\partial\mathcal{L}}{\partial\dot{\alpha}} - \frac{\partial\mathcal{L}}{\partial\alpha} &= -b_\alpha\dot{\alpha} + \tau_{C\alpha}\end{aligned} \tag{1}$$

For our friction model here we must make a simplifying assumption to avoid having to estimate internal constraint forces. In a correct model to handle static friction correctly if the joint angle, $\dot{\theta}$ or $\dot{\alpha}$ is 0, then we must estimate the torque exerted on the joint attempting to overcome static friction. This torque can really be thought of as the constraint torque required to keep the angle fixed, but our Lagrange method sacrifices knowledge of these constraint forces to simplify the equation of motion. To avoid having to estimate this constraint torque we make a simplifying assumption. We only consider the external torques acting on each joint, rather than the internal forces at the joint. These external torques are known, simply the motor torque, τ_m for the horizontal arm and the torque exerted by gravity on the pendulum τ_g.

$$\tau_g = gm_2 l_{2c} \sin(\alpha)$$

With this assumption we can use our previous coulomb friction model with no change. Note that we again use two different frictional torques for the horizontal arm because our previous experiments with the motor discovered significant differences in friction in the forwards and reverse directions. The pendulum has been modeled with a single friction torque because we have no reason to believe that the direction of rotation changes friction.

$$\tau_{C\alpha} = \begin{cases} -\tau_g & \text{if } \dot{\alpha} = 0 \text{ and } |\tau_g| < \tau_{F\alpha} \\ -sgn(\tau_g) \cdot \tau_{FA} & \text{if } \dot{\alpha} = 0 \text{ and } |\tau_{motor}| > \tau_{F\alpha} \\ -sgn(\dot{\alpha}) \cdot \tau_{F\alpha} & \text{if } \dot{\alpha} \neq 0 \end{cases}$$

$$\tau_{C\theta} = \begin{cases} -\tau_m & \text{if } \dot{\theta} = 0 \text{ and } 0 \leq \tau_{motor} < \tau_{F\theta F} \\ -\tau_m & \text{if } \dot{\theta} = 0 \text{ and } -\tau_{F\theta R} \leq \tau_m < 0 \\ -sgn(\tau_m) \cdot \tau_{F\theta F} & \text{if } \dot{\theta} = 0 \text{ and } \tau_m > \tau_{F\theta F} \\ -sgn(\tau_m) \cdot \tau_{F\theta R} & \text{if } \dot{\theta} = 0 \text{ and } \tau_m \leq -\tau_{F\theta R} \geq \\ -sgn(\dot{\theta}) \cdot \tau_{F\theta F} & \text{if } \dot{\theta} > 0 \\ -sgn(\dot{\theta}) \cdot \tau_{F\theta R} & \text{if } \dot{\theta} < 0 \end{cases}$$

The right hand side of the equation contains partial derivatives of the Lagrangian, $\mathcal{L}$, which is given below as the difference of the total kinetic energy of the system, T, and the total potential energy of the system V. Using the expressions derived above for the energies of each component of the system we can construct an expression for $\mathcal{L}$ and take partial derivatives

$$\mathcal{L} = T - V = T_1 + T_2 - (V_1 + V_2) = T_1 + T_{2R} + T_{2T} - V_2$$

$$\mathcal{L} = \frac{1}{2}\dot{\theta}^2 \left(I_{1z1} + C_2 \sin^2(\alpha) + I_{2xx} \cos^2(\alpha) + m_2 l_1^2\right) + \frac{1}{2} C_1 \dot{\alpha}^2 + C_3 \dot{\theta}\dot{\alpha} \cos(\alpha) - C_4 \cos(\alpha) + C_4$$

$$C_1 = I_{2zz} + m_2 l_{2c}^2 \qquad C2 = I_{2yy} + m_2 l_{2c}^2 \qquad C_3 = m_2 l_1 l_{2c} - I_{2xz} \qquad C_4 = l_{2c} m_2 g$$

$$\frac{d}{dt}\frac{\partial \mathcal{L}}{\partial \dot{\theta}} = \ddot{\theta}\left(I_{1z1} + C_2 \sin^2(\alpha) I_{2xx} \cos^2(\alpha) + m_2 l_1^2\right) + 2\left(C_2 - I_{2xx}\right)\dot{\theta}\dot{\alpha} \sin(\alpha)\cos(\alpha) + C_3 \ddot{\alpha}\cos(\alpha) - C_3 \dot{\alpha}^2 \sin(\alpha)$$

$$\frac{\partial \mathcal{L}}{\partial \theta} = 0$$

$$\frac{d}{dt}\frac{\partial \mathcal{L}}{\partial \dot{\alpha}} = C_1 \ddot{\alpha} + C_3 \ddot{\theta}\cos(\alpha) - C_3 \dot{\theta}\dot{\alpha}\sin(\alpha)$$

$$\frac{\partial \mathcal{L}}{\partial \alpha} = \dot{\theta}^2\left(C_2 \sin(\alpha)\cos(\alpha) - I_{2xx}\cos(\alpha)\sin(\alpha)\right) - C_3\dot{\theta}\dot{\alpha} sin(\alpha) + C_4 \sin(\alpha)$$

fix centering on this equation and probably the next one

$$\begin{aligned} \ddot{\theta}\left(I_{1z1} + C_2 \sin^2(\alpha) + I_{2xx}\cos^2(\alpha) + m_2 l_1^2\right) + 2(C_2 - I_{2xx})\dot{\theta}\dot{\alpha}\sin(\alpha)\cos(\alpha) \\ + C_3 \ddot{\alpha}\cos(\alpha) - C_3\dot{\alpha}^2\sin(\alpha) = -b_\theta \dot{\theta} + \tau_m + \tau_{C\theta} \end{aligned} \tag{2}$$

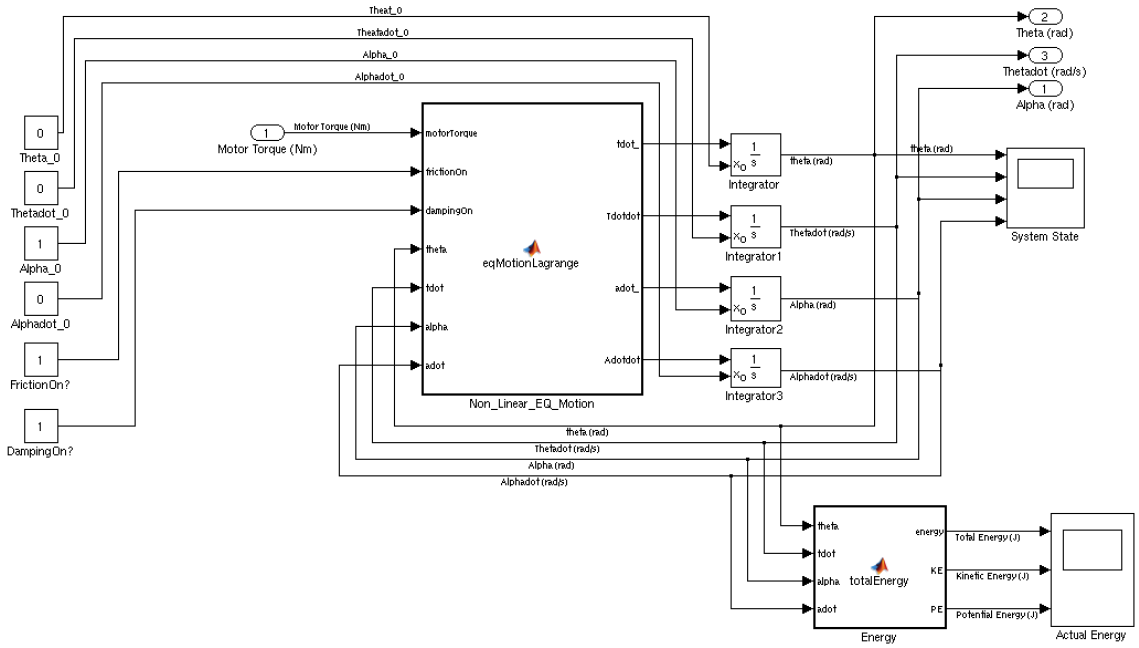

Figure 2: Block Diagram of Non-Linear System Model

$$C_1\ddot{\alpha} + C_3\ddot{\theta}\cos(\alpha) - (C_2 - I_{2xx})\dot{\theta}^2\sin(\alpha)\cos(\alpha) - C_4\sin(\alpha) = -b_\alpha\dot{\alpha} + \tau_{C\alpha} \tag{3}$$

The pair of non-linear differential equations can be used to numerically model the behavior of the system, but they are not particularly useful for actual controller design. Both state space controls and our traditional techniques require the system to be linearized around a particular operating point. This allows us to generate a transfer function to approximate the behavior of the system and lets us construct root locii and bode plots to quantify system behavior.

Electrical Driver and Motor Model

We also modeled the effects of motor back emf which serves to limit the maximum angular velocities that the arm can achieve. For the given command current, we compute the back emf across the motor according to its present angular velocity, $\dot{\theta}$ and the back-emf constant K_b, and compare the required supply voltage with the actual supply voltage, V_s. If the supply voltage is insufficient, we use the supply voltage and the back-emf to compute the voltage across the motor and from that compute the actual motor current. Otherwise motor current is directly proportional to command voltage.

d.

See figure 2 for the block diagram of the non-linear model within Simulink. See the included code in the Appendix for the implemented functions.
add matlab code to Appendix

e.

Linearized Equations of Motion

We will linearize the equations of motion about $\theta = 0$, $\alpha = 0$. By taylor expansion about this point and dropping higher order terms we obtain:

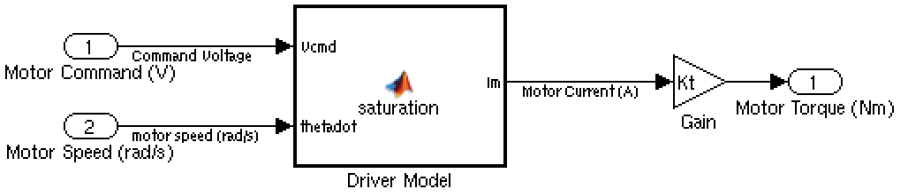

Figure 3: Block Diagram of Driver and Electrical Motor Model

$$\sin(\alpha) \approx 0 \qquad \cos(\alpha) \approx \alpha \qquad \sin(\theta) \approx 0 \qquad \cos\theta \approx \theta$$

We note that the coulomb friction terms from the previous non-linear equations must be dropped completely as there is no reasonable linearization of the effects of friction. We also note that we expect $\dot{\theta}$ and $\dot{\alpha}$ to be relatively small, which implies:

$$\dot{\theta}\dot{\alpha} \approx 0$$

Applying these to equations (2) and (3) yields (4) and (5) respectively.

$$\ddot{\theta}\left(I_{1z1} + I_{2xx} + m_2 l_1^2\right) + \ddot{\alpha}C_3 = -b_\theta\dot{\theta} + \tau_m \tag{4}$$

$$\ddot{\alpha}C_1 + \ddot{\theta}C_3 - \alpha C_4 = -b_\alpha\dot{\alpha} \tag{5}$$

Using equations (4) and (5) together we can generate two independent equations for $\ddot{\alpha}$ and $\ddot{\theta}$.

$$C_5 = (I_{1z1} + I_{2xx} + m_2 l_1^2)$$

$$\ddot{\theta} = \frac{C_3 b_\alpha\dot{\alpha} - C_3 C_4\alpha - C_1 b_\theta\dot{\theta} + C_1\tau_m}{C_5 C_1 - C_3^2} \tag{6}$$

$$\ddot{\alpha} = \frac{-C_5 b_\alpha\dot{\alpha} + C_3 b_\theta\dot{\theta} + \alpha C_4 C_5 - C_3\tau_m}{C_5 C_1 - C_3^2} \tag{7}$$

State Space Model

State Space Representation models a dynamical system as a set of linear, time-varying differential equations. What is known as the state of the system is a set of variables, the generalized coordinates, q_i that completely describe the internal state of the system. For the inverted pendulum we choose the coordinates:

$$\mathbf{X}(t) = [q_1(t), q_2(t), q_3(t), q_4(t)]^T = [q_1(t), \dot{q}_1(t), q_3(t), \dot{q}_3(t)]^T = [\theta(t), \dot{\theta}(t), \alpha, \dot{\alpha}(t)]^T$$

In this generalized coordinate system, we compute the derivative of the state, $\dot{X}$ as a function of the current state $\mathbf{X}$ and the inputs $\mathbf{u}$.

$$\dot{\mathbf{X}}(\mathbf{t}) = [\dot{q}_1(t), \dot{q}_2(t), \dot{q}_3(t), \dot{q}_4(t)]^T = [\dot{q}_1(t), \ddot{q}_1(t), \dot{q}_3(t), \ddot{q}_3(t)]^T = [\dot{\theta}(t), \ddot{\theta}(t), \dot{\alpha}(t), \ddot{\alpha}(t)]^T$$

Because our system is linear this relationship can be related through the State Matrix A and the Input Matrix B which map the current state and external inputs into the system into the change in state through the following equation.

$$\dot{\mathbf{X}}(t) = A(t)\mathbf{X}(\mathbf{t}) + B(t)\mathbf{u}(t)$$

$$A_{ij} = \frac{\partial \dot{q}_j}{\partial q_i}(t) \qquad B_i = \frac{\partial \dot{q}_i}{\partial u_i}(t)$$

The actual output that we wish to control is determined from $\dot{\mathbf{X}}(t)$ and from the inputs $\mathbf{u}(t)$ through the Output Matrix, $C(t)$ and the Direct Transmission Matrix $D(t)$. Then our output $\mathbf{Y}(t)$ can be represented as follows:

$$\mathbf{Y}(t) = C(t)\dot{\mathbf{X}}(t) + D(t)\mathbf{u}(t) = C(t)\left\{A(t)\mathbf{X}(\mathbf{t}) + B(t)\mathbf{u}(t)\right\} + D(t)\mathbf{u}(t)$$

As noted above the matrices A, B, C, and D may in general be functions of time, however because our system is time invariant, these matrices become independent of time. The notation below has been simplified accordingly. The matrices A and B may be obtained directly from our linearized equations of motion above.

need to format this matrix to look better

$$A = \begin{bmatrix} \frac{\partial \dot{\theta}}{\partial \theta} & \frac{\partial \dot{\theta}}{\partial \dot{\theta}} & \frac{\partial \dot{\theta}}{\partial \alpha} & \frac{\partial \dot{\theta}}{\partial \dot{\alpha}} \\ \frac{\partial \ddot{\theta}}{\partial \theta} & \frac{\partial \ddot{\theta}}{\partial \dot{\theta}} & \frac{\partial \ddot{\theta}}{\partial \alpha} & \frac{\partial \ddot{\theta}}{\partial \dot{\alpha}} \\ \frac{\partial \dot{\alpha}}{\partial \theta} & \frac{\partial \dot{\alpha}}{\partial \dot{\theta}} & \frac{\partial \dot{\alpha}}{\partial \alpha} & \frac{\partial \dot{\alpha}}{\partial \dot{\alpha}} \\ \frac{\partial \ddot{\alpha}}{\partial \theta} & \frac{\partial \ddot{\alpha}}{\partial \dot{\theta}} & \frac{\partial \ddot{\alpha}}{\partial \alpha} & \frac{\partial \ddot{\alpha}}{\partial \dot{\alpha}} \end{bmatrix} = \begin{bmatrix} 0 & 1 & 0 & 0 \\ 0 & \frac{\partial \ddot{\theta}}{\partial \dot{\theta}} & \frac{\partial \ddot{\theta}}{\partial \alpha} & \frac{\partial \ddot{\theta}}{\partial \dot{\alpha}} \\ 0 & 0 & 0 & 1 \\ 0 & \frac{\partial \ddot{\alpha}}{\partial \dot{\theta}} & \frac{\partial \ddot{\alpha}}{\partial \alpha} & \frac{\partial \ddot{\alpha}}{\partial \dot{\alpha}} \end{bmatrix}$$

$$\frac{\partial \ddot{\theta}}{\partial \ddot{\theta}} = -\frac{C_1 b_\theta}{C_5 C_1 - C_3^2} \qquad \frac{\partial \ddot{\theta}}{\partial \alpha} = -\frac{C_3 C_4}{C_5 C_1 - C_3^2} \qquad \frac{\partial \ddot{\theta}}{\partial \dot{\alpha}} = \frac{C_3 b_\alpha}{C_5 C_1 - C_3^2}$$

$$\frac{\partial \ddot{\alpha}}{\partial \dot{\theta}} = \frac{C_3 b_\theta}{C_5 C_1 - C_3^2} \qquad \frac{\partial \ddot{\alpha}}{\partial \alpha} = \frac{C_4 C_5}{C_5 C_1 - C_3^2} \qquad \frac{\partial \ddot{\alpha}}{\partial \dot{\alpha}} = -\frac{C_5 b_\alpha}{C_5 C_1 - C_3^2}$$

$$B = \begin{bmatrix} \frac{\partial \dot{\theta}}{\partial \tau_m} \\ \frac{\partial \ddot{\theta}}{\partial \tau_m} \\ \frac{\partial \dot{\alpha}}{\partial \tau_m} \\ \frac{\partial \ddot{\alpha}}{\partial \tau_m} \end{bmatrix} = \begin{bmatrix} 0 \\ \frac{C_1}{C_5 C_1 - C_3^2} \\ 0 \\ -\frac{C_3}{C_5 C_1 - C_3^2} \end{bmatrix}$$

We wish to stabilize the pendulum vertically, so the output be are interested in is precisely $\alpha(t)$. Thus C becomes simply:

$$C = [0, 0, 1, 0]^T$$

For this system, the only external input, the motor torque $\tau_m(t)$, does not directly influence the output, $\mathbf{Y}(t)$ except for its influence on $\dot{\mathbf{X}}(t)$ making D simply the zero matrix.

$$D = [0, 0, 0, 0]^T$$

System Transfer Functions

To generate the transfer functions it is more straight forwards to proceed from equations (4) and (5) than from (6) and (7). Applying the Laplace transform (4) and (5) yields and performing arithmetic operation to isolate $\theta(s)$ and $\alpha(s)$ yields the following transfer functions from motor torque, $\tau(s)$ to $\theta(s)$ and $\alpha(s)$ respectively.

$$\frac{\theta(s)}{\tau_m(s)} = \frac{s^2 C_1 + s b_\alpha - C_4}{\left(s^2 C_1 + s b_\alpha - C_4\right)\left(s^2 C_5 + s b_\theta\right) - s^4 C_3^2} \tag{8}$$

$$\frac{\alpha(s)}{\tau_m(s)} = \frac{-s^2 C_3}{\left(s^2 C_1 + s b_\alpha - C_4\right)\left(s^2 C_5 + s b_\theta\right) - s^4 C_3^2} \tag{9}$$

If we were to neglect the effects of damping, then (8) and (9) would reduce to the following:

$$\frac{\theta(s)}{\tau_m(s)} \approx \frac{s^2 C_1 - C_4}{s^2 \left[s^2 \left(C_5 C_1 - C_3^3\right) - C_4 C_5\right]}$$

$$\frac{\alpha(s)}{\tau_m(s)} \approx \frac{-s^2 C_3}{s^2 \left[s^2 \left(C_5 C_1 - C_3^3\right) - C_4 C_5\right]}$$

In the simplified transfer function for $\alpha(s)$ above it appears as if we can cancel the but this not the case as we see when we examine equation (9).

2 Parameter Identification

The inverted pendulum system includes many parameters related to the mechanical and electrical properties of the system. To determine these, we used a combination of manufacturer data sheets, CAD modeling, physical measurements, and experimental regression.

Most of the relevant motor parameters were previously determined in the DC motor lab. In that case, most of the parameters were provided by the manufacturer, but we performed regression on experimental data to fit our model with the test data and found that the true values were different from those on the data sheet. The relevant values are shown in table 1. An abbreviated except from our DC motor lab is given below to show our procedure for determining these values.

	Data-Sheet Values	Fit Values
J_{motor} $\left(\frac{N \cdot s^2}{m}\right)$	$8.5 \cdot 10^{-6}$	$3.50514 \cdot 10^{-5}$
K_t $\left(\frac{N \cdot m}{A}\right)$	0.0424	0.0314499
$b_{forwards}$ $(N \cdot s)$	$3.7 \cdot 10^{-6}$	$1.08586 \cdot 10^{-5}$
$b_{reverse}$ $(N \cdot s)$	$3.7 \cdot 10^{-6}$	$4.85930 \cdot 10^{-5}$
$\tau_{forwards}$ $(N \cdot m)$	$5.6 \cdot 10^{-3}$	0.0224389
$\tau_{reverse}$ $(N \cdot m)$	$5.6 \cdot 10^{-3}$	0.0143096

Table 1: DC Motor Final Parameter Values vs Original Data Sheet Values

To determine the parameters of the motor we used MATLAB's numerical differential equation solving to simulate the trajectory of the system as a function of time, driver current, I_t and our unknown system parameters J, b, K_t, and $\tau_{coulomb}$. By then comparing the predicted angular positions with the measured angular positions over time, we can construct a non-linear regression to estimate the unknown parameters. We collected a data set where the driver was given a sinusoidal voltage, and we assume that motor current, I_m, is identical to this driver voltage and recorded the motor motion that this input caused.

With this model and some intelligent guessing for new parameter values, we arrived at an excellent fit shown in figure 4. The most notable feature of these values is the large difference between the torque of friction in the forwards and reverse directions.

With the motor parameters largely known already, we focused on determining the parameters of the new components comprising the pendulum and horizontal arm. To ensure accuracy, we used multiple methods and compared results. For example, all of the mass of every component was determined on the scale provided in the mechatronics lab. We then built CAD models of every component in SolidWorks using a combination of engineering drawings, physical measurements, and already built models from McMaster-Carr. By setting the material properties correctly, SolidWorks can determine the mass of every part. We compared this calculated value to the measured values and they all matched within the limits of resolution of the scale. This gave us confidence in the ability of SolidWorks to calculate the other necessary parameters.Therefore, we built assemblies of the pendulum, the horizontal arm and complete system, and we used SolidWorks to calculate the masses, centers of mass, and moments of inertia that we needed. Figures 5, 6, and 7 show the CAD assemblies. The inertia matrix for the pendulum and other relevant values are given below. Note that the axes labels in the SolidWorks models are not the same as those in our derived equations.

$$\begin{vmatrix} \bar{I}_{xx} & \bar{I}_{xy} & \bar{I}_{xz} \\ \bar{I}_{yx} & \bar{I}_{yy} & \bar{I}_{yz} \\ \bar{I}_{zx} & \bar{I}_{zy} & \bar{I}_{zz} \end{vmatrix}_{Pendulum} = \begin{vmatrix} 8.1 \cdot 10^{-6} & 2.03 \cdot 10^{-5} & 0 \\ 2.03 \cdot 10^{-5} & 3.711 \cdot 10^{-4} & 0 \\ 0 & 0 & 3.646 \cdot 10^{-4} \end{vmatrix}$$

Translating from the coordinate system established in Solid Works to our coordinate system yields the following moment of inertia tensor:

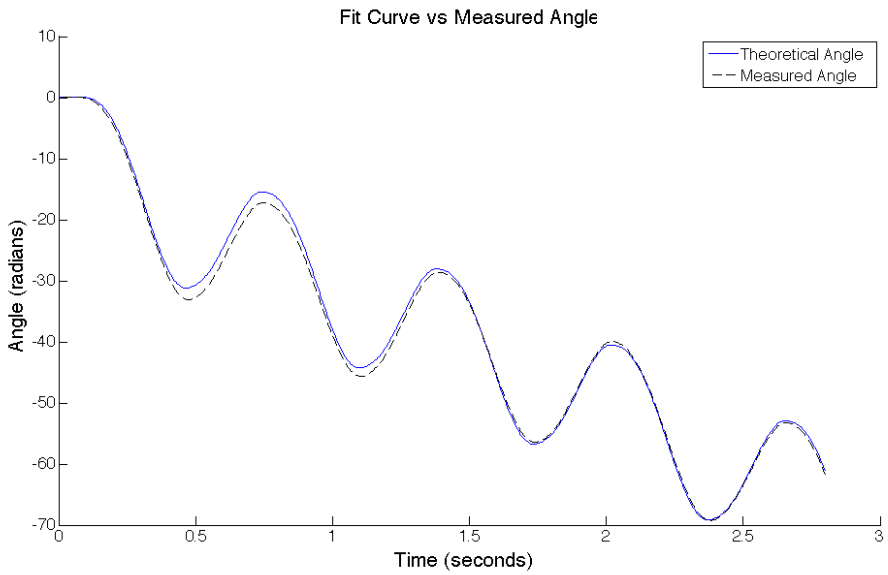

Figure 4: Predicted behavior vs Actual behavior using fit parameter values and enhanced modeling

$$I_2 = \begin{bmatrix} 8.1 \times 10^{-6} & 0 & 2.03 \times 10^{-5} \\ 0 & 3.711 \times 10^{-4} & 0 \\ 2.03 \times 10^{-5} & 0 & 3.646e{-}4 \end{bmatrix} kg \cdot m^2$$

$$m_1 = 0.1481kg \quad m_2 = 0.0820kg$$

$$l_1 = 0.10826m \quad l_{2C} = 0.08568m$$

$$I_{1zt} = \left(6.78 \times 10^{-4} + 3.50514 \times 10^{-5}\right)\ kg \cdot m^2 = 7.1305 \cdot 10^{-4} kg \cdot m^2$$

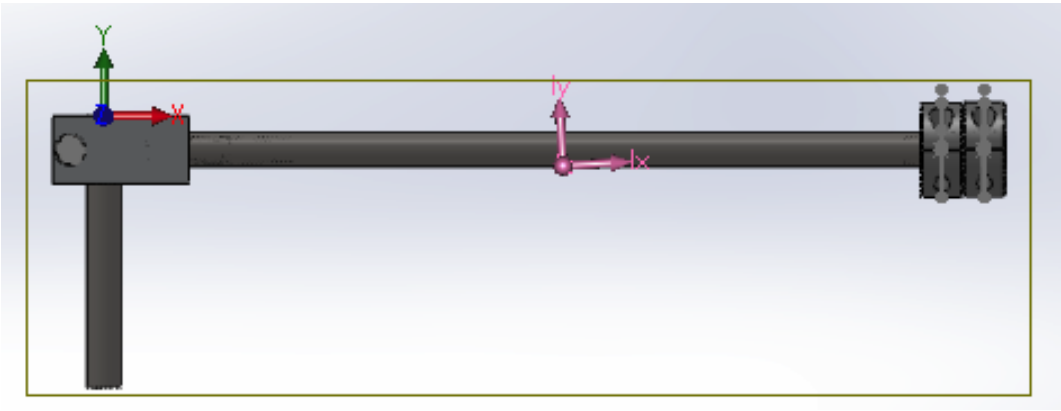

Figure 5: SolidWorks Model of Pendulum

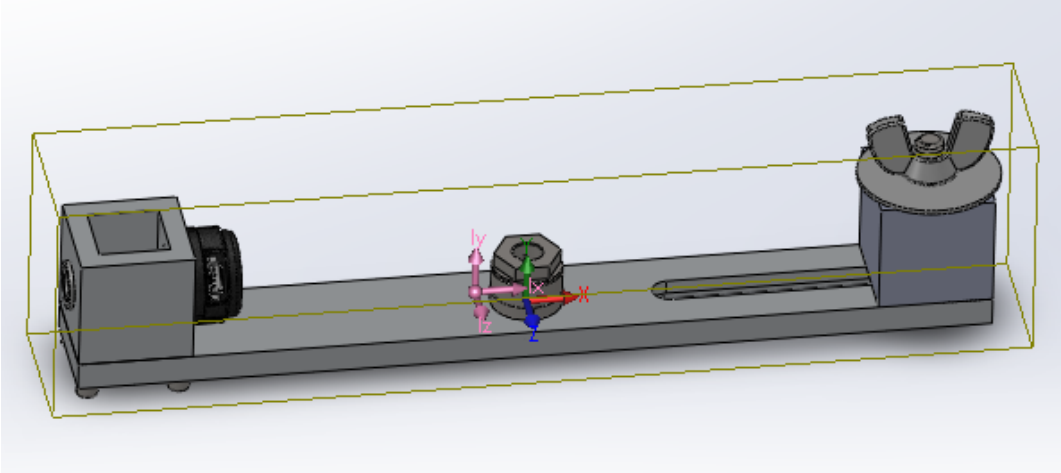

Figure 6: SolidWorks Model of Horizontal Link

For the pendulum we assume that frictional torque, $\tau_{F\alpha}$, and the viscous damping coefficient, b_α to be the same in each direction. These terms for the pendulum were estimated in an experiment where the horizontal arm was fixed in place and the pendulum was allowed to swing freely from an initial angle. By comparing the decaying envelope, extracted as the maximum and minimum of each oscillation, of the actual system motion with a similar plot generated from a simulated model, we formed a rough estimate of these terms.

$$b_\alpha = 6.5 \cdot 10^{-6}\, N \cdot s \qquad \tau_{F\alpha} = 7.0 \cdot 10^{-6}\, N \cdot m$$

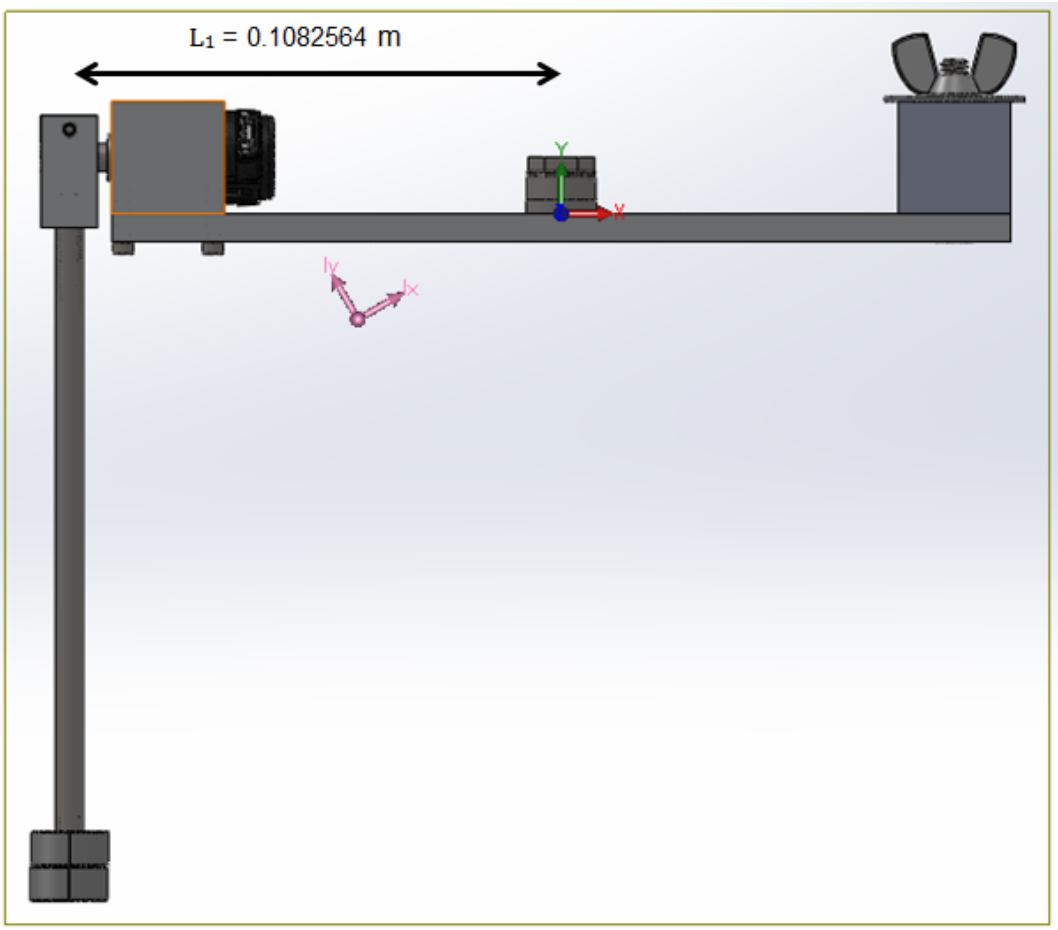

Figure 7: SolidWorks Model of Assembled Pendulum and Horizontal Link

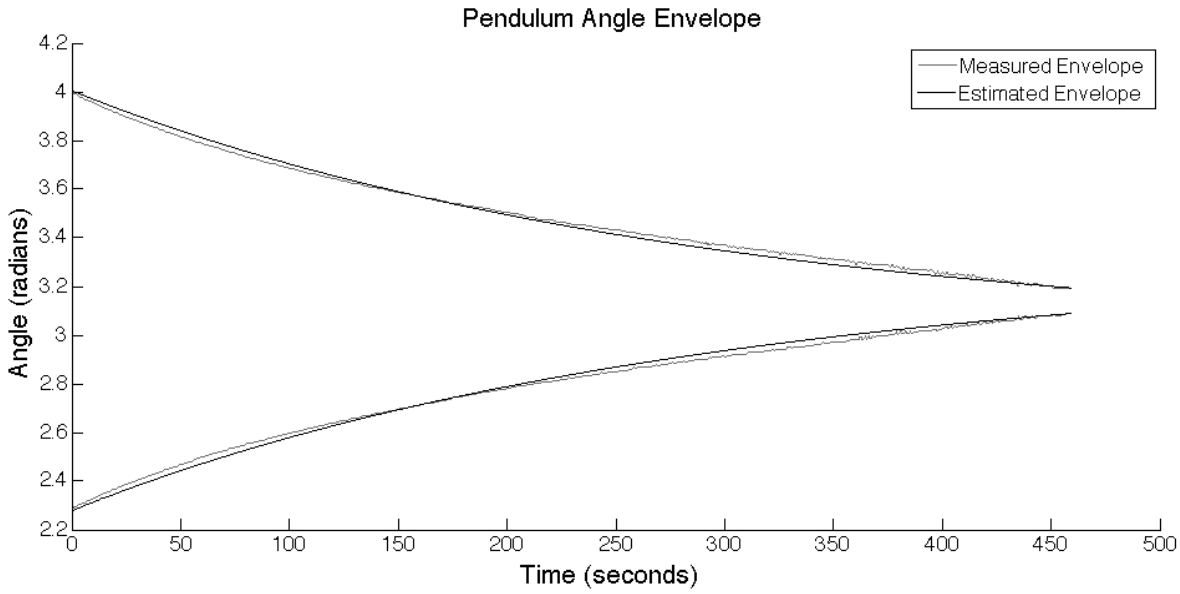

Figure 8: Actual Decaying Envelope of motion vs Simulated Envelope

3 Comparing Linear and Non-Linear Models

Figures 9 and 10 show the pendulum and horizontal arm angle response from the nonlinear model compared to experimental data. The data was obtained by allowing the pendulum to oscillate freely from a starting angle and then running the simulink model with the same initial conditions. The predicted pendulum angle agrees with the experimental data quite well for the first few periods, but quickly deviates. Interestingly, after several periods the experimental angle doesn't decay as quickly as the predicted angle, but the decay accelerates after several more periods and the pendulum comes to rest much sooner in the real system than in the model. A possible cause of this is the force applied by the encoder cable on the horizontal arm, which is unmodelled and very nonlinear and unpredictable. This is especially apparent in figure 10, where the horizontal arm prediction and real behavior were very far off.

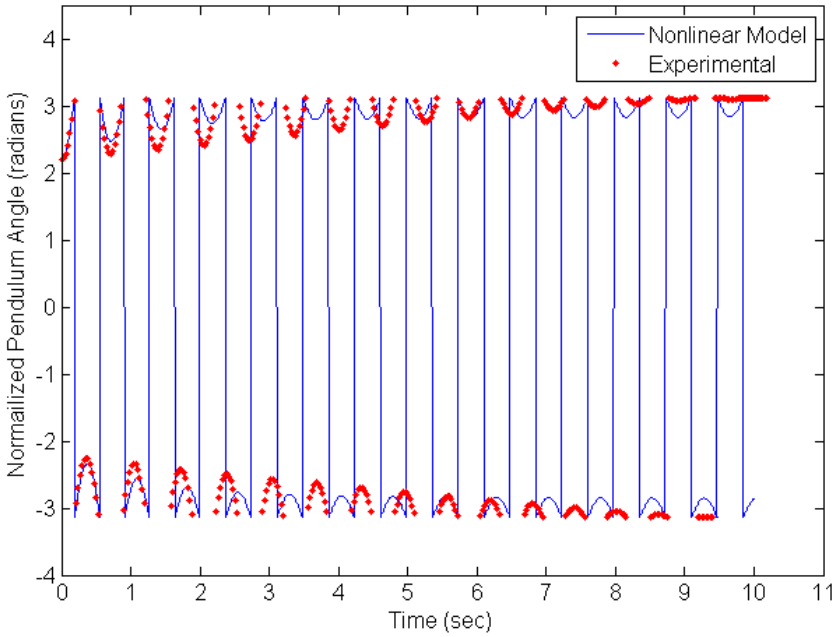

Figure 9: Comparison of Normalized Pendulum Angle From the Nonlinear Model and Experimental Data

Figures 11 and 12 show the pendulum and horizontal arm angle response from the linearized model compared to experimental data. The predicted pendulum angle agrees with the experimental quite well for several periods. Somewhat surprisingly, the linear model matches the experimental data longer than the nonlinear model did. However, the linear model decays extremely slowly. This is largely because the friction terms are no longer present, and friciton on the horizontal arm played a large role in reducing the energy of the system. While the linear pendulum angle seems to perform reasonably well initially, the linear horizontal arm angle does not agree with the test data at all. If the angle data was not normalized, the predicted arm angle in figure 12 would grow without bound. A possible cause of this is that our linear model does not incorporate all of the friction and damping forces that act on the horizontal arm, and the encoder cable applies significant resistance to rotation on the arm.

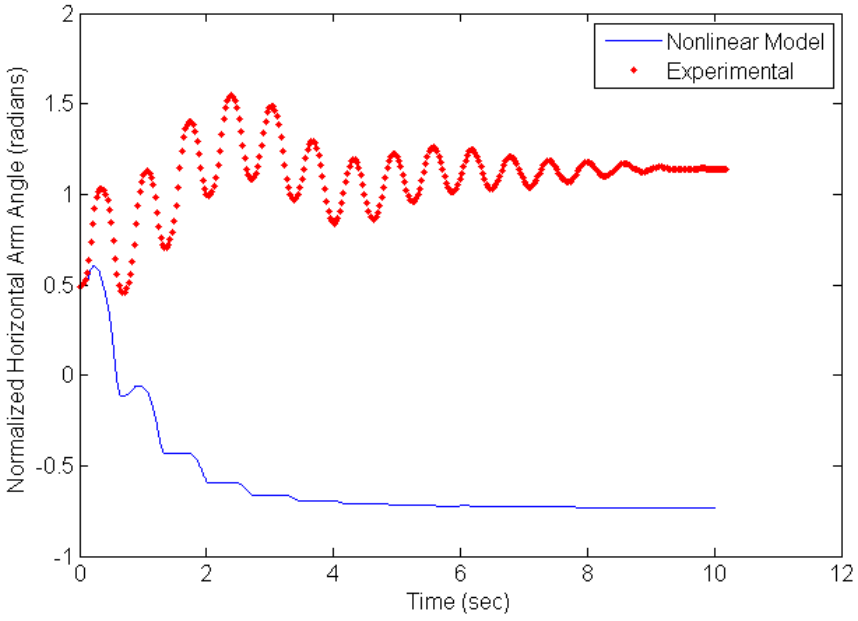

Figure 10: Comparison of Normalized Horizontal Arm Angle From the Nonlinear Model and Experimental Data

To investigate the effect that the encoder cord has on the system, we ran tests with the cable removed. This meant that we could only get data on the horizontal arm angle. To ensure consistency, we raised the pendulum to a horizontal position before releasing it, then ran the simulink model from a horizontal starting position. Figure 13 shows the results of such a test. The initial transient phase of the two datasets still doesn't agree, and the real system decays much slower, but it's interesting that both move towards +-π (though the normalization of the angles makes this somewhat hard to see). This suggests to us that the cord is having a large effect on the system, but there are other factors which haven't been considered (such as tilt of the table).

Figure 14 shows the predicted pendulum angle from the nonlinear model and from the linearized model. Just as when comparing both models to the experimental data, there is some agreement in the first few periods, but then the two models diverge. This is largely because the lack of friction in the linearized model causes it to decay much more slowly. There is also a noticeable phase difference as time increases because the nonlinear model predicts a slightly longer period of oscillation.

It is clear that there are weakness in the linear model based on the weak agreement with the nonlinear model and real system. However, this is largely because the linearization assumptions are based on the pendulum being very close to the vertical equilibrium point for use with a balancing controller. While we linearized the system about the bottom position for the purposes of comparing to the test data, the assumptions that the small angle theorem would hold and that $\dot{\theta}$ and $\dot{\alpha}$ would be small were not necessarily true when in a free swinging situation instead of being balanced. Therefore, we believe that our linearization assumptions are valid as long as we only apply the linearization within a small angle range and have a balance controller active to minimize $\dot{\theta}$ and $\dot{\alpha}$. The greatest effect of the linearization was the dropping of the friction terms (which was more of a practical necessity rather than an assumption). This had a large effect on the decay of the systems oscillations, but with our balance controller active, this assumption should not have a significantly negative effect.

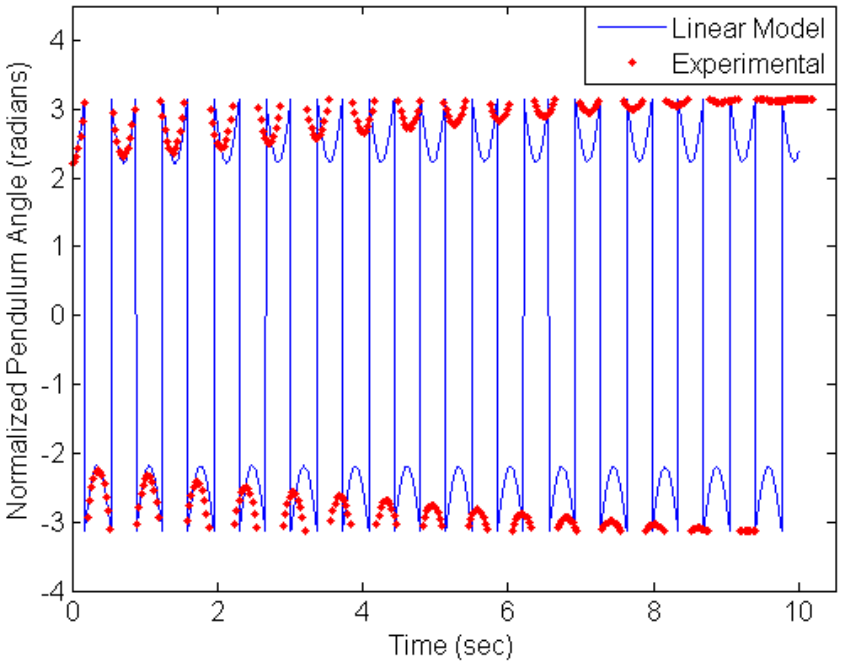

Figure 11: Comparison of Normalized Pendulum Angle From the Linearized Model and Experimental Data

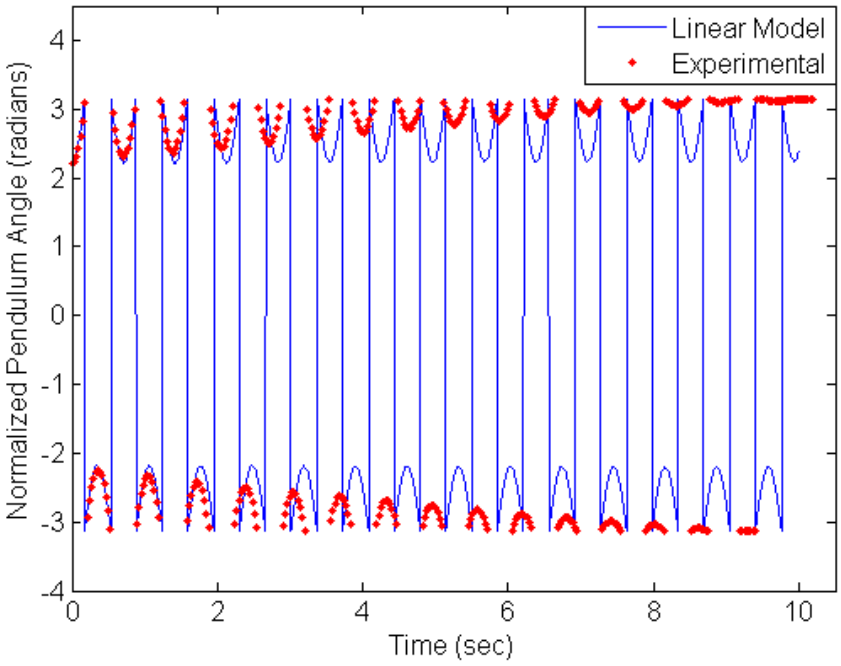

Figure 12: Comparison of Normalized Horizontal Arm Angle From the Linearized Model and Experimental Data

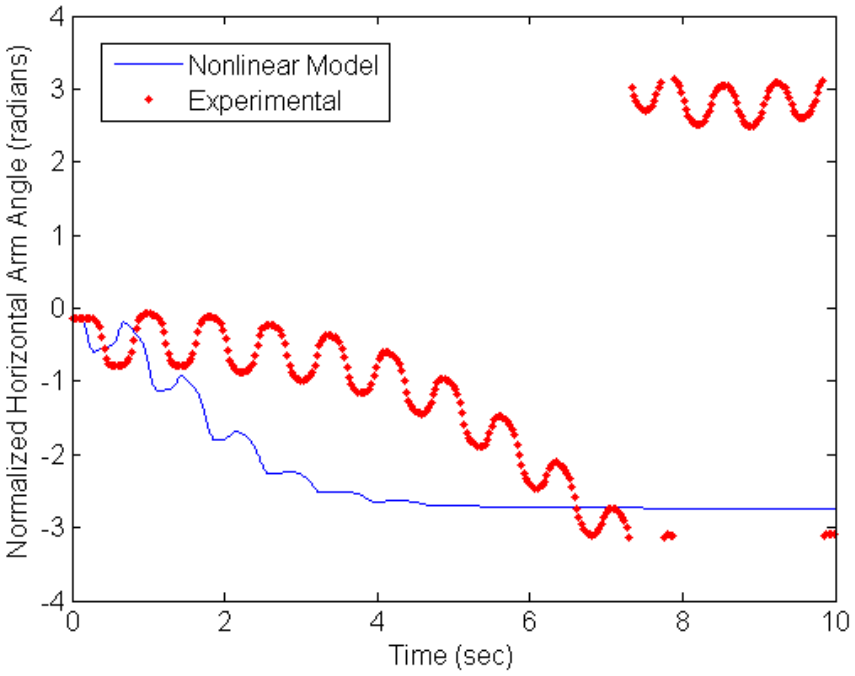

Figure 13: Comparison of Normalized Horizontal Arm Angle From the Nonlinear Model and Experimental Data with the Encoder Cable Removed

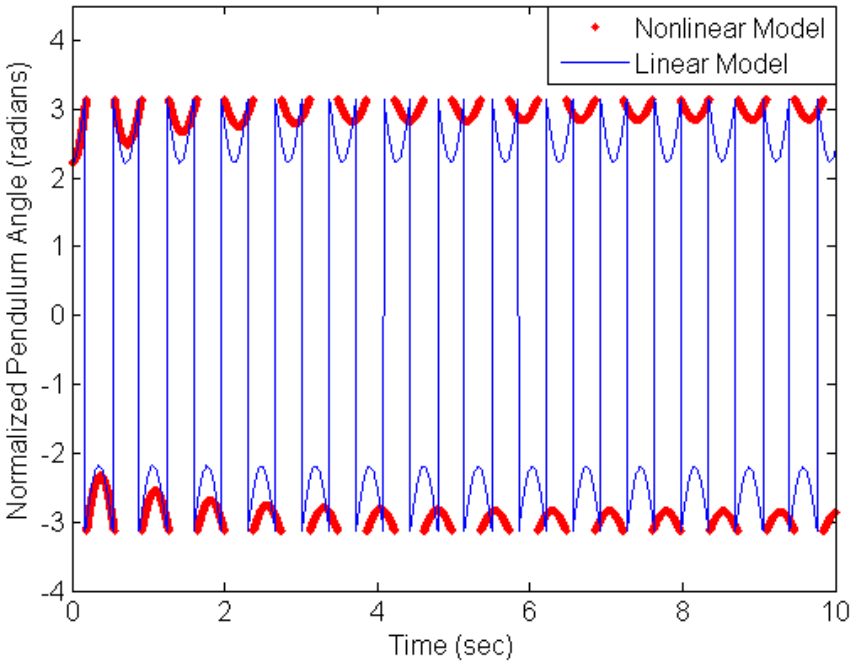

Figure 14: Comparison of Normalized Pendulum Angle From the Nonlinear Model and Linearized Model

4 State Space Controls in Simulink

Using the A, B, C, and D matrices derived earlier together with the tuned Q and R matrices below, we constructed a full-state feedback controller using the Matlab *lqr* function.

$$Q = \begin{bmatrix} 10 & 0 & 0 & 0 \\ 0 & 40 & 0 & 0 \\ 0 & 0 & 120 & 0 \\ 0 & 0 & 0 & 60 \end{bmatrix} \qquad R = [6]$$

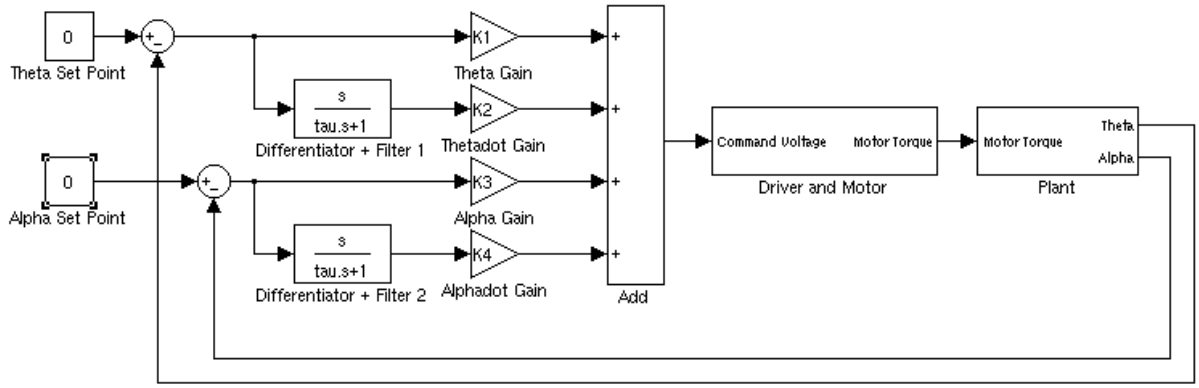

Figure 15: Block Diagram of State Space Balancing Controller

$$K_1 = -1.2910 \qquad K_2 = -2.9161 \qquad K_3 = -66.3961 \qquad K_4 = -8.4496$$

The full-state feedback controller using the gains above successful stabilized both of our linear and non-linear models. The effects of disturbing the system with an angle of 0.1 radians is shown in figures 16 and 17. Figure 16 compares the response of the linear system to the response of the non-linear model. The most obvious difference between both responses is the significantly larger oscillations present in the linear system although each system shows similar behavior. We note in the α response that the linear model overshoots the set point angle before returning to the set point angle over a long period of about 0.6 seconds. The non-linear model on the other hand shows very little overshoot at all and settles in under 0.2 seconds. However the controller has difficulty returning θ to the set point in the non-linear model taking approximately 10 seconds to return to 0.

Figure 17 introduces frictional forces to the non-linear model. Here we note that the system remains stable, but θ is unable to return to its set-point settling at 0.545 radians after about 10 seconds.

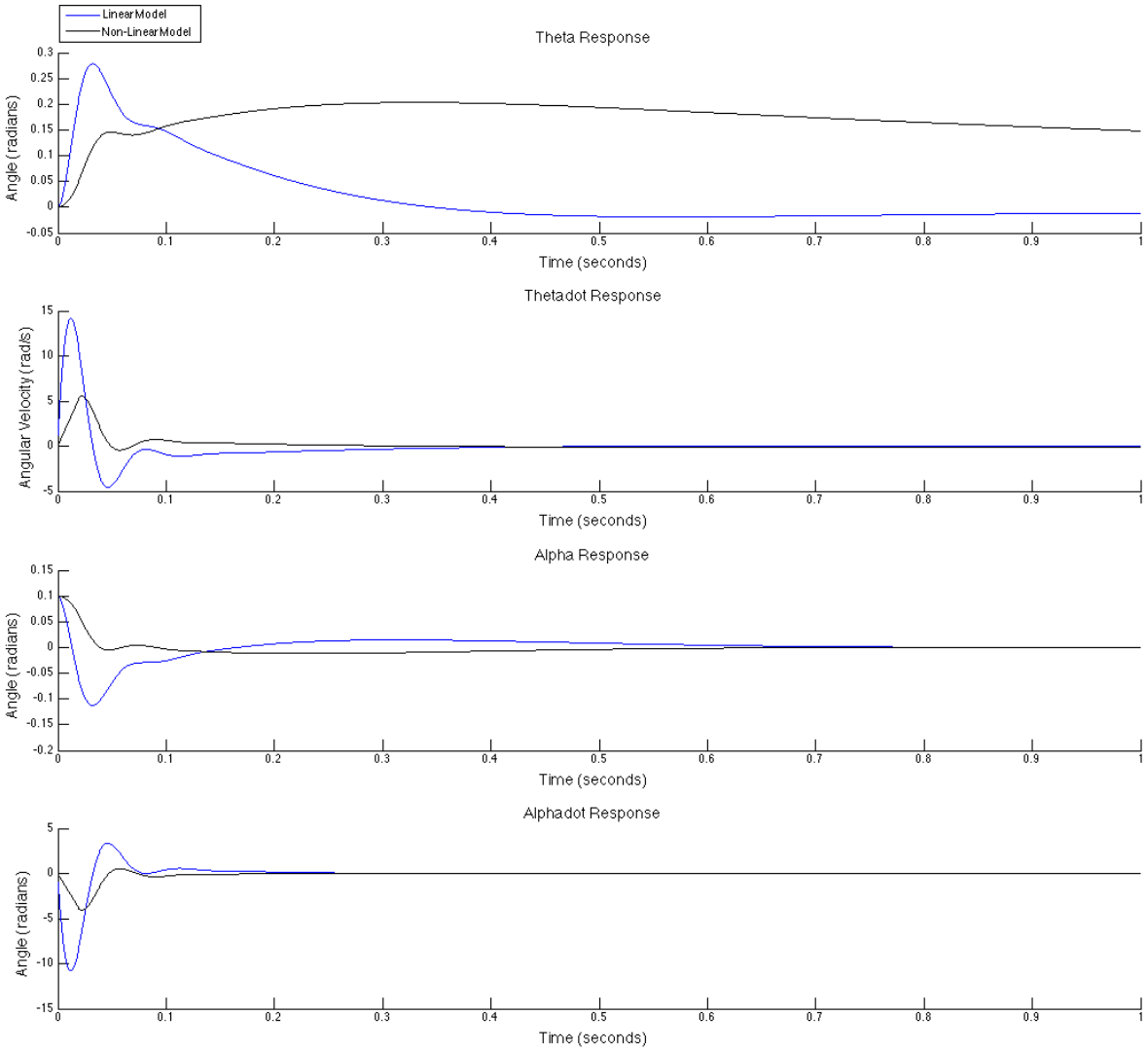

Figure 16: Comparison of Balancing controller response to perturbation, $\alpha_0 = 0.1$, for Linear and non-Linear models

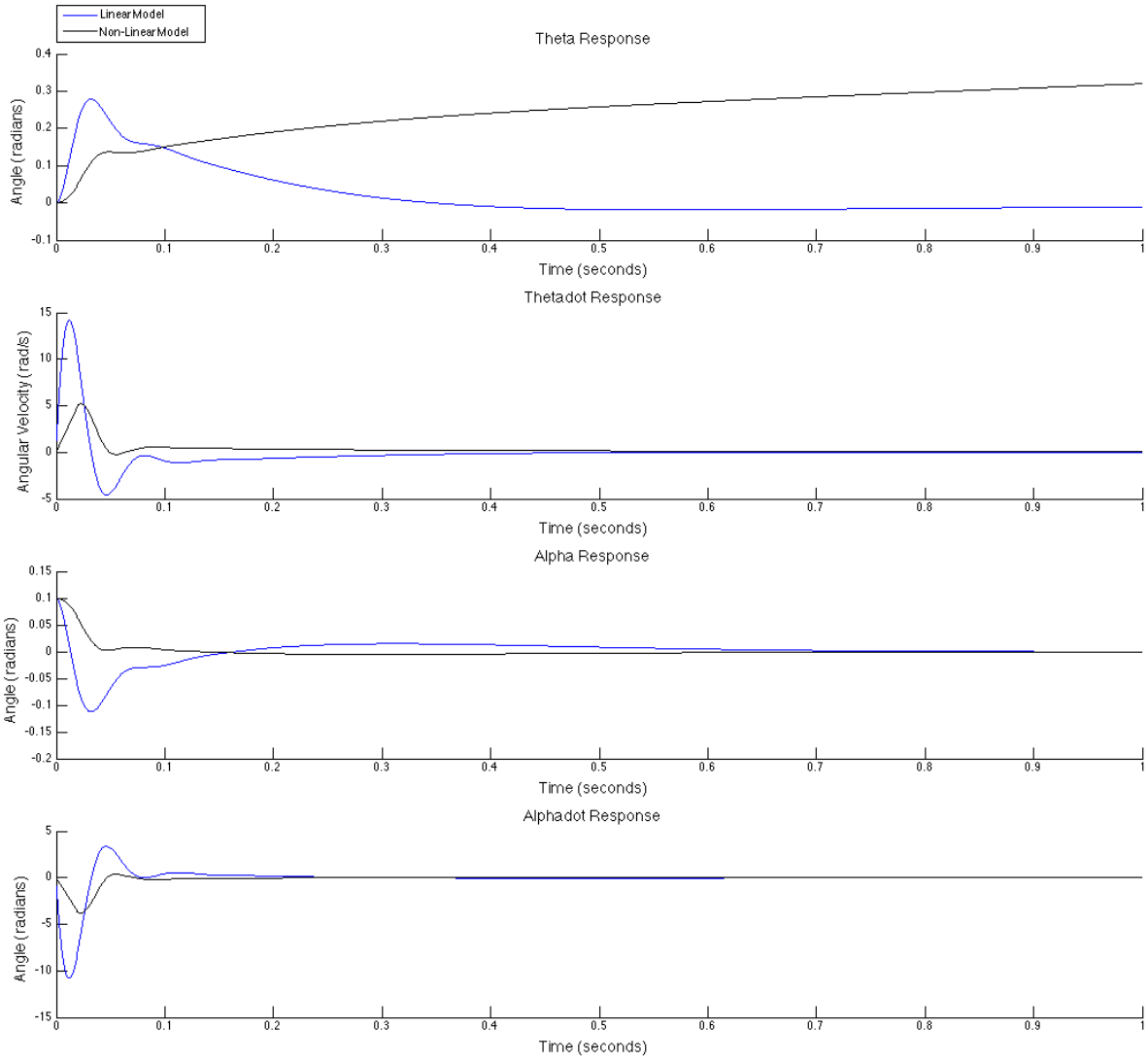

Figure 17: Comparison of Balancing controller response to perturbation, $\alpha_0 = 0.1$, for Linear and non-Linear models including effects of friction in the non-Linear Model

5 Swing Up Controller in Simulink

6 LabView Implementation

a.

Angle normalization was implemented using the $mod2\pi()$ function. The function works by limiting an input angle, θ to $\pm\pi$ radians which effectively represents the entire angular spectrum of 2π radians. The advantage of using $mod2\pi()$ over a function that normalizes θ from 0 to 2π is that the angular reset point is at $\pm\pi$ as opposed to 0 radians. For our inverted pendulum we would like to ensure that α and θ are close to zero. Using $mod2\pi()$ ensures that spikes do not occur about the transition point.

The code for the $mod2\pi$ operation is as follows:

```
if t<0
    t = -t;
    sign = -1;
else
    sign = 1;
tout = sign*(t - floor(t*0.5/pi + 0.5) * 2 *pi);
```

θ is represented as t. For our normalization, we require t to be positive and we keep track of the original sign of t through the variable *sign*. *tout* represents the output value of $mod2\pi(\theta)$. The $floor$ operation essentially finds the quotient of dividing t by 2π and the the $+0.5$ operation allows the angle to be normalized between $+\pi$ on one side and $-\pi$ on the other. This way, we can constrain θ to stay between $\pm\pi$.

$mod2\pi$ is very useful for controlling α. α will reach its unstable equilibrium every 2π radians and we are happy with it as long as the pendulum balances in the unstable equilibrium. Additionally the change from $+\pi$ to $-\pi$ occurs when the the pendulum is facing downwards, but at this point the swing-up controller would be operational and for the swing-up controller, the sign of $\cos(\alpha)$ in the $+\pi$ and $-\pi$ quadrants are the same, so this does not affect the system.

For θ control we have to be a little careful - the horizontal arm moves a lot during swing up and generally during balancing as well, if we apply a $mod2\pi()$ operation before calculating $\dot{\theta}$, the derivative will spike up violently during the $\pm\pi$ crossover point - this in turn would destabilie the inverted pendulum system. Hence it is a good idea to calculate $\dot{\theta}$ from θ_{Absolute}.

In general it is good practice to use a $mod2\pi()$ operation on repetitive angular functions, it helps in numerical precision in trigonometric functions also captures the nature of the system - after a point, we get back to where we were.

b.

While implementing the system in Labview we used the Matlab script block which allowed us to write Matlab code for execution as opposed to creating a messy wire-block diagram. The front panel and the block diagram can be seen in figure 18.

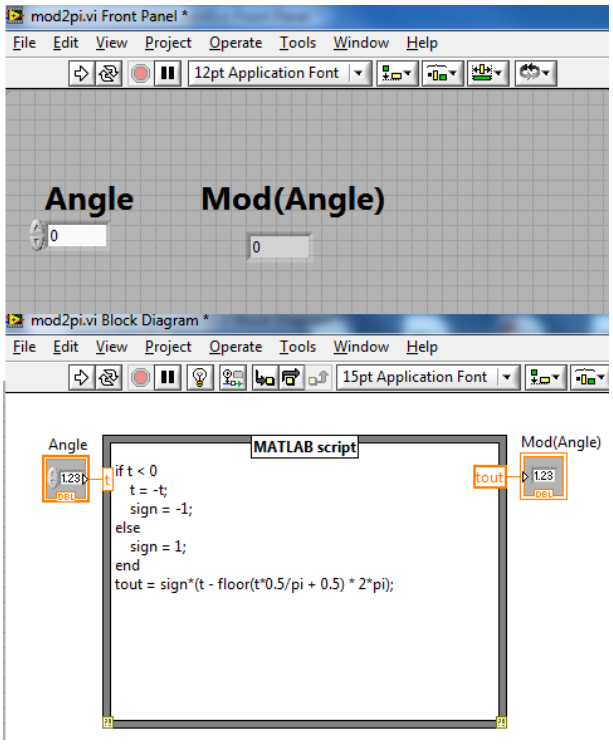

Figure 18: Front panel and block diagram of $mod 2\pi$.

c.

d.

7 Effects on LabView Loop Rate on Stability

8 Classical Controller

9 Another Swing Up Controller

10 Parasitic Effects

Appendix.

Add matlab code and stuff here